ELSEVIER

Surface Science 350 (1996) 11–20

surface science

Growth of ultrathin Pd films on Al(001) surfaces

V. Shutthanandan [1], Adli A. Saleh, N.R. Shivaparan, R.J. Smith *

Physics Department, Montana State University, Bozeman, MT59717, USA

Received 25 September 1995; accepted for publication 3 November 1995

Abstract

High-energy ion backscattering spectroscopy (HEIS) and X-ray photoelectron spectroscopy (XPS) were used to determine the growth mode and the interface structure of ultrathin Pd films deposited on Al(001) surfaces at room temperature. Measured Al and Pd surface peak areas for MeV He^+ ions incident normal to the surface show that Pd atoms intermix with and displace Al substrate atoms. The mixing continues for Pd coverages from 0–5 monolayers, at which point a Pd metal film begins to grow on the alloy surface. XPS measurements of the Pd 3d photopeaks show a chemical shift that is consistent with the formation of an AlPd-like compound during the mixing phase, and Pd metal thereafter. HEIS results further reveal that the alloyed overlayer as well as the Pd metal film have some degree of axial alignment with respect to the Al substrate. The XPS intensity measurements are consistent with this two-stage growth model.

Keywords: Aluminum; Epitaxy; High energy ion scattering (HEIS); Metal–metal interfaces; Palladium; Single crystal surfaces; X-ray photoelectron spectroscopy

1. Introduction

The interaction of thin films of transition metals with aluminum surfaces has attracted increasing attention in recent years because of potential technological applications such as high-temperature, low-density structural materials, catalysis, and metalization layers on semiconductors [1,2]. For example, the growth modes of ultrathin Ti, Ni and Fe films on single-crystal aluminum surfaces have been studied to understand the role of the substrate geometry and other factors in the evolution of the transition metal–aluminum interface [3–5]. Saleh and co-workers [3] have shown that ultrathin Ti films grow epitaxially on the Al(110) and Al(001) surfaces up to 5 monolayers (ML) of Ti coverage. In previous publications we have reported results for the growth of ultrathin Ni films on Al(110) and Al(001) surfaces which show that Ni films grow differently on these two substrates at room temperature [4]. Since Ni and Pd have similar bulk equilibrium phase diagrams with Al [6], and at the same time they belong to the same group in the periodic table, we might expect the behavior of Pd thin films on Al single crystal surfaces to be similar to that for the Al–Ni system.

Initially, it was reported that Pd grows in a Stranski–Krastanov mode on Al(111) surfaces [7], that is, islands of Pd grow on top of a single layer of Pd atoms covering the Al surface. A layer-by-layer growth mode was reported for Pd on Al(110)

* Corresponding author. Fax: +1 406 994 4452; e-mail: smith@physics.montana.edu.

[1] Present Address: Electric Propulsion Laboratory, Department of Mechanical Engineering, Tuskegee University, Tuskegee, AL 36088, USA.

PII 0039-6028(95)01117-X

surfaces [8]. However, using medium energy ion scattering studies, Smith and co-workers have shown that considerable mixing occurs between Pd and Al atoms when Pd thin films are deposited on both Al(111) and (110) surfaces [9]. Their Al(111) results suggest that an AlPd-like alloy grows on the substrate with sufficient order to allow subsequent epitaxial growth of Pd(111) on the AlPd alloy. It has also been reported that the β-AlPd compound always forms as the initial reaction product in Al–Pd bilayer experiments [10]. However, it was also reported that Al_3Pd was the first compound to form in thermally reacted Al–Pd bilayers [11]. In light of these conflicting observations, the Al–Pd system merits more study.

To better characterize the evolution of the Al/Pd interface we have carried out high-energy ion scattering (HEIS) and X-ray photoelectron spectroscopy (XPS) experiments on thin Pd films deposited on Al(001) single crystal surfaces at room temperature. HEIS is used primarily to characterize the growth mode and the interface structure, while XPS is used to identify the chemical state of the interface. In addition, HEIS is used to measure the overlayer coverage accurately. The results reported here show that Pd atoms intermix with surface Al atoms up to 5 monolayers (ML) of Pd coverage, at which point a Pd metal film begins to cover the surface alloy.

2. Experimental setup

The experiments were performed in an ultrahigh vacuum (UHV) chamber with a base pressure of 1×10^{-10} Torr. A detailed description of the experimental setup can be found in Refs. [4,12]. Briefly, the system consists of a vacuum chamber which is attached to a 2 MV Van de Graaff accelerator via a differentially pumped beamline, and includes facilities for performing high-energy ion scattering and X-ray photoelectron spectroscopy experiments. The He ion energy used in the HEIS measurements was about 1 MeV. The channeling measurements were made with the ion beam incident along the [001] direction. A solid-state detector was used to collect the backscattered He ions at a scattering angle of 105°. The typical dose of incident He ions for one spectrum was 1.6×10^{15} ions/cm^2. The XPS spectra were acquired using an Al-K_α X-ray source and a 100 mm hemispherical analyzer. The analyzer was operated in the fixed-analyzer-transmission mode with a pass energy of 50 eV. For XPS measurements the sample was kept in the channeling alignment and the photoelectrons entered the analyzer with a polar emission angle of 30° from the sample normal. All XPS binding energies presented in this work are referenced to the binding energy of the clean Al 2p core level. Initially, the Al single crystal was cleaned using the methods described in Ref. [4]. The typical cleaning procedure in vacuum involved successive cycles of argon ion sputtering with 1.5 keV ions followed by annealing to 450°C. Surface cleanliness was verified by XPS and HEIS. Palladium was vapor deposited onto the Al(001) surface from a resistively heated Pd wire. The source consisted of 3 strands of 0.25 mm diameter Pd wire (99.997% purity) twisted and then wound into a coiled filament. The typical deposition rate with a filament current of 4.25 amps was about 0.5 ML/min. No increase of sample temperature was observed during evaporation. After each Pd deposition HEIS and XPS experiments were performed. In the HEIS experiment the surface peak areas (SPA) for ions backscattered from Al and Pd atoms were monitored. For each Pd deposition on the Al(001) surface the coverage of Pd (atoms/cm^2) was calculated using the SPA for Pd, the Rutherford cross section, and the HEIS experimental parameters. The uncertainty in the results reported here is estimated to be 5.6%, with the largest contribution to the uncertainty coming from the determination of the detector solid angle, and smaller contributions coming from uncertainties in the integrated charge, the scattering angle, and the determination of the surface peak area. In the XPS measurements Al 2p and Pd 3d core level spectra were collected in the same manner as described in Ref. [4].

3. Results

In Fig. 1 we show the energy distribution of the backscattered He ions in the regions of the Al and

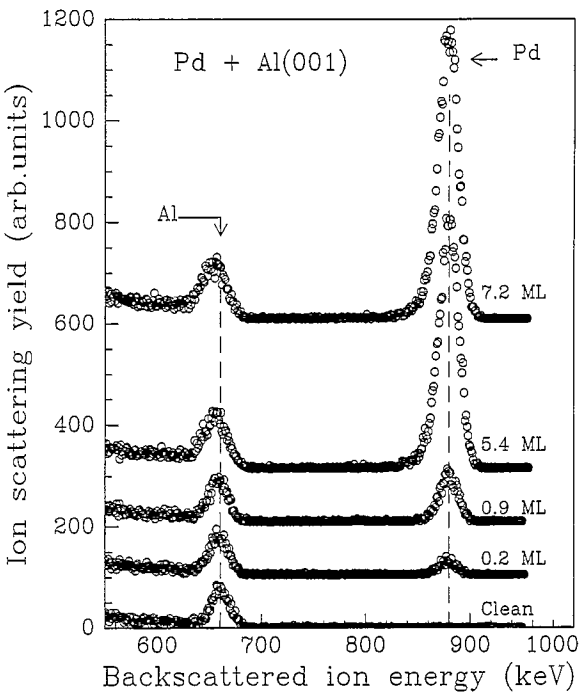

Fig. 1. Ion backscattering spectra for 1 MeV He^+ ions on Pd+Al(001) for different Pd coverages indicated in the figure. The energetic positions of the Al and Pd surface peaks are indicated by the arrows and the dashed lines.

Pd surface peaks for several Pd coverages. Each curve in Fig. 1 is identified by the Pd coverage. One monolayer here is equivalent to the atomic density of the Al(001) plane, 1.219×10^{15} atoms/cm^2. The arrows and the dashed lines in the figure indicate the energetic positions expected for ions backscattered from Al and Pd atoms at the surface. It can be seen from the figure that the surface peak area for Al increases with increasing Pd coverage. This indicates that more Al atoms are visible to the ion beam in the presence of Pd atoms at the surface. That is, surface Al atoms have moved from their initial equilibrium positions and have reduced the shadowing of substrate Al atoms. If on the other hand the Pd atoms formed an overlayer directly above the Al atoms, we would expect to see a reduction in the SPA of Al associated with Pd shadowing of Al atoms, similar to the behavior measured for Ti films on Al surfaces [3]. Thus, this observation of an increase in the SPA rules out the formation of an ordered Pd overlayer at lattice sites directly above Al surface atoms.

In Fig. 2 we plot the number of Al atoms visible to the incident ion beam (Al SPA) as a function of Pd coverage (Pd SPA) as determined from channeling spectra similar to those shown in Fig. 1. Such plots are very helpful for developing models for alloyed interfaces, as demonstrated by us and others [4,5,13]. There are two main regions to note in this figure. First, the Al surface peak area exhibits a linear increase with a slope of 1 up to 5 ML of Pd coverage. After this coverage, there is an apparent saturation stage during which the Al surface peak area remains unchanged. A similar plot of the number of Pd atoms visible to the incident ion beam in the normal-incidence channeling direction as a function of Pd coverage is shown by the open circles in Fig. 3. The actual Pd coverage is measured with the ion beam incident in a random direction so as to avoid any Pd–Pd shadowing. The solid circles in Fig. 3 show the Pd yields for ions incident in the random direction. A small but measurable amount of Pd shadowing is observed for coverages greater than 1.5 ML as seen by the reduction in the Pd yields obtained in the normal-incidence channeling direction as compared to that obtained for the random direction of incidence.

Fig. 4 is a plot of the X-ray photoelectron energy distribution curves for the Pd $3d_{5/2}$ (binding energy 335.08 eV) and Pd $3d_{3/2}$ photopeaks for three different coverages of Pd on Al(001). The solid curves through the data are the results from the peak shape analysis discussed in this paper. The arrows in the figure indicate the photopeak positions for the AlPd compound and Pd metal phases. A background of secondary electrons has been subtracted from these data, and the spectra have been shifted vertically to facilitate a comparison of the curves. From these figures, one can unambiguously see that the line shape of the Pd peak changes as Pd coverage on the surface increases.

4. Discussion

The results of Figs. 1 and 2 suggest that more and more Al atoms become visible to the incident

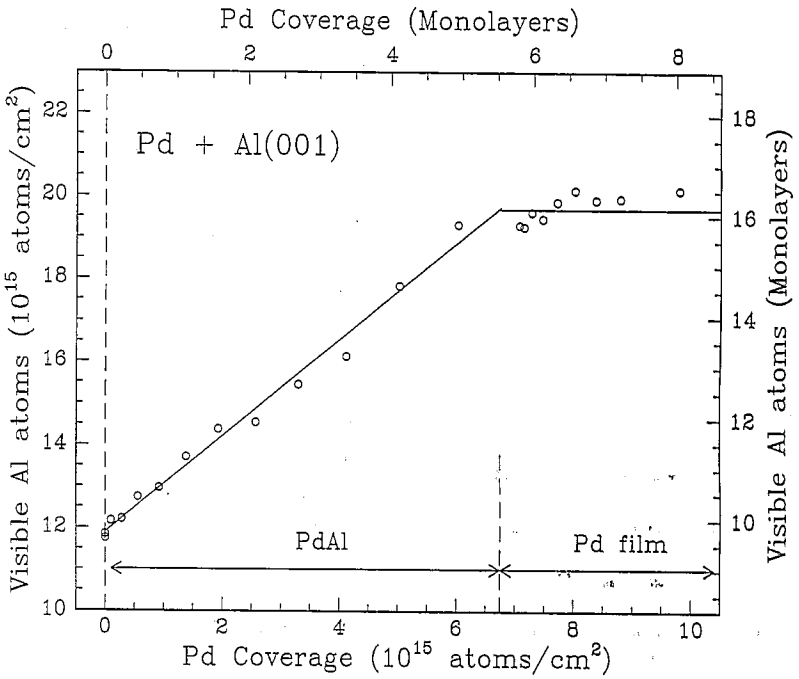

Fig. 2. Number of Al atoms visible to the incident ion beam as a function of Pd coverage on the Al(001) surface. The solid lines are the least-squares fit to the data points in two regions. Two different stages of film growth are indicated.

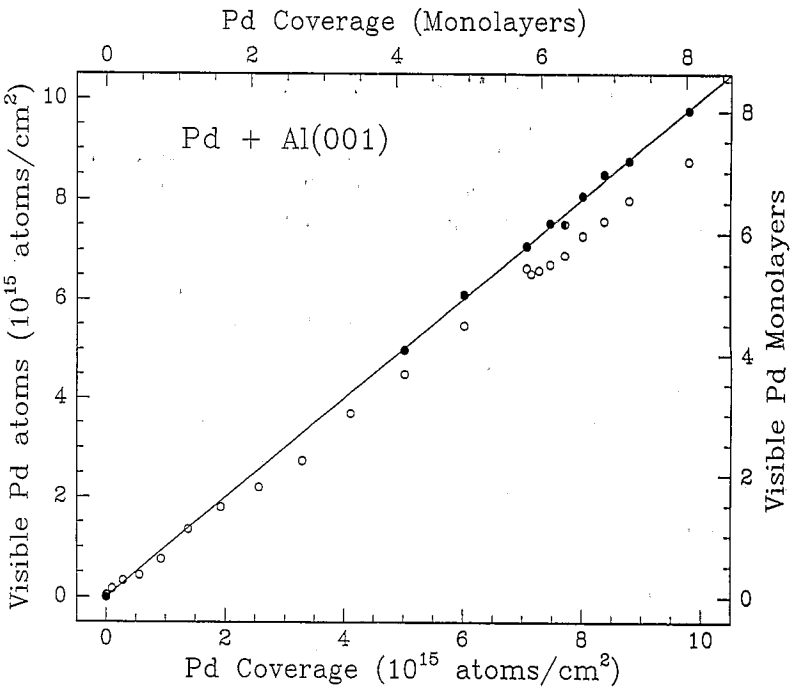

Fig. 3. Number of Pd atoms visible to the incident ion beam as a function of Pd coverage. The solid circles are for a random incidence direction and the open circles are for the channeling direction. The solid line is the least-squares fit to the random data.

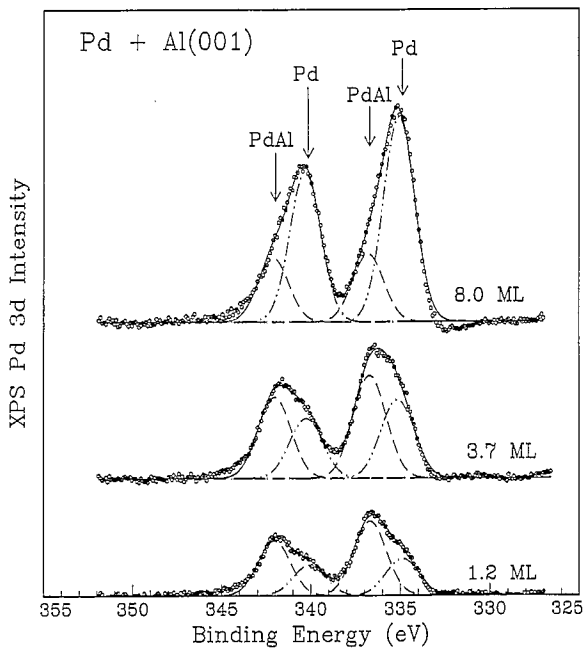

Fig. 4. Pd 3d XPS spectra from Pd films deposited at room temperature on the Al(001) surface for three different Pd coverages. The solid curves are the results of the XPS peak fittings. The dashed lines represent the contributions from Pd photoelectrons originating from the AlPd alloy and the dotted lines represent the contributions from Pd photoelectrons originating from the Pd metal. Peak positions expected for the AlPd compound and for Pd metal are indicated by arrows.

ion beam as the Pd coverage increases up to 5 ML. We conclude that Pd atoms are mixing with Al atoms on the Al(001) surface to form a surface alloy. For the bottom three curves shown in Fig. 1 the Al surface peak position is essentially the same as for the clean Al surface. That is, we did not observe any shift in the Al surface peak, even after 4.5 ML of Pd deposition. However, after this coverage of Pd, the surface peak position of Al starts shifting gradually towards lower energies as seen from the top two curves in Fig. 1. This shift cannot be attributed solely to the small energy loss of the He ions as they pass through the thin layer of Pd at the surface of the alloy ($\approx$0.65 keV per monolayer of Pd). It may also be the result of dechanneling of the ions in the near-surface region of the Al substrate. The relatively heavy Pd atoms can act as scattering centers at the surface and slightly alter the He ion trajectories. This causes additional ions to collide with substrate atoms in a region below the surface, but not sufficiently deep to be distinguished energetically from surface scattering events. Consequently, the surface peak area increases, and there is a small shift of the peak to lower energies depending on the relative amount of near-surface dechanneling [14]. It is seen in Fig. 1 that the low-energy tail of the Pd surface peak is broadened at 7.2 ML of Pd coverage as compared to that for 0.9 ML and 5.4 ML. This suggests that a very small amount of Pd atoms (less than 0.5 ML) have diffused deeper into the Al bulk at room temperature. The presence of these Pd atoms in the Al bulk leads to slight deflections of some He ions, and increases the backscattering yield from Al atoms in the substrate, as seen by the increase in the minimum yield behind the Al surface peak in Fig. 1. On the other hand, since we did not observe any significant broadening of the Pd peak at coverages less than 5 ML, and continuous displacements of the Al atoms are observed for these lower Pd depositions, we infer that the deposited Pd atoms are staying near to the surface region, resulting in alloy formation at the surface for these coverages.

In a conventional interpretation of the results in Fig. 2, the slope for ion scattering yield versus Pd coverage is used to determine the average stoichiometry of the surface alloy. In this case a slope of unity for low Pd coverages would indicate that an AlPd compound is forming at the surface. However, such an interpretation must be made with caution as we have shown for the case of Ni on Al(110) where near-surface dechanneling resulted in a larger slope than expected for the NiAl compound [14]. Nevertheless, based on the XPS results discussed below, we conclude that an AlPd surface compound is formed for Pd coverages less than 5 ML. So, at least in this case, both the HEIS results and the XPS results agree quite well. Furthermore, the AlPd compound has the highest heat of formation and is the most stable phase in the Al–Pd phase diagram, so we might expect it to form first [6]. In previous studies of Pd on Al(111) surfaces, Smith and co-workers reported that the AlPd surface compound is the initial reaction product on that surface. Their conclusion

was based primarily on the medium energy ion scattering studies [9].

After 5 ML of Pd coverage the deposited Pd atoms are not effectively displacing the Al atoms as seen from the zero slope of Al yield versus Pd coverage in region two of Fig. 2. This means that at these higher coverages the mixing seems to stop and, in agreement with the XPS results discussed below, a Pd metal film begins to cover the surface. The measured ion scattering yield from Pd atoms, plotted in Fig. 3, further suggests that the surface alloy and the Pd film have some degree of axial alignment with respect to the Al substrate. This conclusion is based on the observation of Pd–Pd or Al–Pd shadowing for Pd coverages greater than 2 ML. The small amount of shadowing (about 10%) could result from the formation of small Pd islands aligned normal to the Al surface.

By performing a detailed peak shape analysis of the Pd 3d XPS photopeaks shown in Fig. 4 we can identify the compound growing at the Al–Pd interface. In this figure the Pd peak shape changes with Pd coverage. At low Pd coverage the Pd $3d_{5/2}$ and Pd $3d_{3/2}$ peaks are centered near 336.75 and 342.05 eV, respectively (bottom curve in Fig. 4). The peaks show a small shoulder on the low binding energy side. However, at larger Pd coverages the spectra display peaks at 335.08 and 340.28 eV, respectively (top curve in Fig. 4). These shifts in the Pd peaks suggest that the photoelectrons originating from the Pd atoms are experiencing a different chemical environment in these two coverage regimes. The main peak seen at lower coverages is attributed to Pd photoelectrons originating from the mixed Al–Pd interface. The small shoulder in this curve is explained by the fact that the area of the sample imaged by the analyzer lens with the aperture used in our system is slightly larger than the Al crystal so that a small portion of the sample holder is also seen by the analyzer. This means that the XPS spectrum of Pd includes a small amount of Pd signal coming from the sample holder in addition to the signal originating from the sample. The Pd metal on the Mo sample holder appears to have little or no chemical shift relative to bulk Pd metal, as seen from Fig. 4. The main photopeak which we observe at higher coverages is attributed to photoelectrons originating from Pd metal on the sample and on the sample holder.

In order to reduce this sample size problem, and to determine the overlayer morphology, we have carried out a detailed peak shape analysis of the Pd peaks. Initially, a cubic background is removed from the original XPS curves. We then fit the peaks with four different Gaussian line shapes, each with the same peak width. Two Gaussian line shapes were used to represent the Pd $3d_{5/2}$ and Pd $3d_{3/2}$ photopeaks from the Pd metal, and the other two line shapes were intended to represent the Pd $3d_{5/2}$ and Pd $3d_{3/2}$ peaks from the Al–Pd surface alloy. The amplitudes and the peak positions of the fitting functions were allowed to vary in the fitting routine. The dashed lines and the dotted lines in Fig. 4 show the results of our XPS curve fitting.

The fitted curves shown in Fig. 4 clearly indicate a contribution from the Al–Pd alloy as well as from Pd metal. Fuggle and coworkers have studied in detail the chemical shifts of the Pd 3d photopeaks in various Al–Pd alloys [15]. They found that the Pd 3d photopeaks exhibit very large chemical shifts, on the order of 2 eV towards higher binding energies, in the Al–Pd alloys. Their results are summarized in Table 1. The results obtained from our XPS curve fittings are also presented in Table 1. From the table we see that our measured value of the chemical shift and the separation between the Pd $3d_{5/2}$ and Pd $3d_{3/2}$ peaks agree quite well with Fuggle's value for the AlPd compound, and are significantly different from those for the Al_3Pd compound. That is, the chemical shift in the Pd peaks of the AlPd alloy in Fuggle's experiment is equal to 1.9 eV, while in our case it is equal to 1.73 eV. The small difference observed in these values may be associated with the different forms of samples used in these experiments. In Fuggle's experiments the XPS spectra were measured for pure bulk Al–Pd alloys while we collected XPS spectra for very thin films of the Al–Pd compound. The observation of a slightly smaller chemical shift in our experiment is attributed to the emission of photoelectrons from very thin AlPd films for which the charge transfer from Pd to Al

Table 1
Comparison of binding energies, chemical shift and peak separation for the Pd $3d_{5/2}$ and $3d_{3/2}$ photopeaks in different Al–Pd alloys; the chemical shifts are averaged over both 3d lines for the purpose of comparing with Ref. [15]

Compound	Binding energy $3d_{5/2}$ (eV)	Binding energy $3d_{3/2}$ (eV)	Chemical shift (eV)	Separation between $3d_{5/2}$–$3d_{3/2}$ (eV)
Pd metal (Ref. [15])	335.2	340.45	–	5.25
Pd metal (this work)	335.08	340.28	–	5.20
AlPd (Ref. [15])	337.05	342.35	1.9	5.30
AlPd (this work)	336.75	342.05	1.73	5.30
Al_3Pd (Ref. [15])	337.70	342.90	2.5	5.20

may be different than that occurring in the bulk alloy. From these observations we conclude that an AlPd-like surface compound forms at the Pd–Al(001) interface up to 5 ML of Pd coverage.

In Fig. 5 we plot the XPS peak areas for the two fitted Pd $3d_{5/2}$ peaks as a function of Pd coverage. The emission intensities from the Pd compound are denoted by open circles (dashed line) while those for the Pd metal are denoted by the solid circles (solid line). Initially, the intensity from the Pd compound increases smoothly with the Pd coverage up to 4 ML, and then starts to attenuate slowly with increasing Pd coverage. On the other hand, the intensity of the Pd metal emission increase linearly with Pd coverage up to 4 ML. After 4 ML of Pd coverage a more rapid

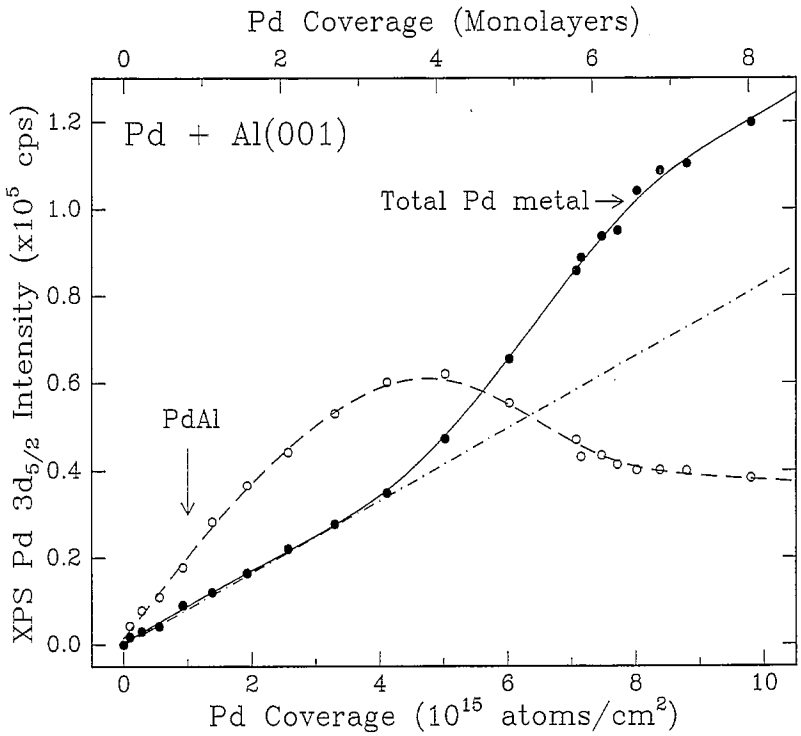

Fig. 5. Measured XPS intensity for the Pd $3d_{5/2}$ photopeak as a function of Pd coverage. The open circles (dashed line) show the intensity for Pd photoelectrons coming from the AlPd alloy. The solid circles (solid line) show the intensity for Pd photoelectrons originating from both the sample and the sample holder. The dashed line shows an approximation for the expected contribution from the sample holder. The lines are provided to guide the eye.

increase in the Pd metal intensity is observed. From these intensity profiles it is clear that at or around 4 ML of Pd coverage a transition occurs in the Pd film growth. These observations can be explained as follows. The initial increase in the Pd metal intensity up to 4 ML of Pd coverage is attributed to the Pd signal coming from the Pd metal on the sample holder. The increase observed in the Pd compound intensity is coming completely from the sample. However, based on the ion scattering results, after 5 ML of Pd coverage we believe that the mixing between the Pd and Al atoms stops and that a Pd metal film begins to grow on the surface alloy. This is consistent with the increase observed in the Pd metal XPS intensity as well as the attenuation observed in the Pd compound intensity. That is, the Pd metal film covering the reacted interface attenuates the Pd signal originating from the interface alloy, and at the same time it causes the Pd metal intensity to increase at a faster rate since more Pd metal atoms are now imaged by the analyzer.

Even after 4 ML of Pd coverage we are still depositing a very small amount of Pd metal onto the sample holder which will continue to contribute to the total Pd metal intensity. In an attempt to remove the signal contribution from the sample holder we assumed that the Pd intensity coming from the holder is not saturated after 4 ML of Pd coverage, but instead increases linearly with Pd coverage. This assumption seems valid because the amount of Pd metal film deposited onto the sample holder is very small, and the attenuation length at these high kinetic energies is quite large. We then subtract this linear increase in the Pd intensity from the total Pd metal intensity. In Fig. 6 we plot the corrected XPS intensities from the Pd and the AlPd compound. The results presented in Fig. 6 show more clearly the onset of Pd metal formation after 4 ML of Pd deposition. The subtraction pro-

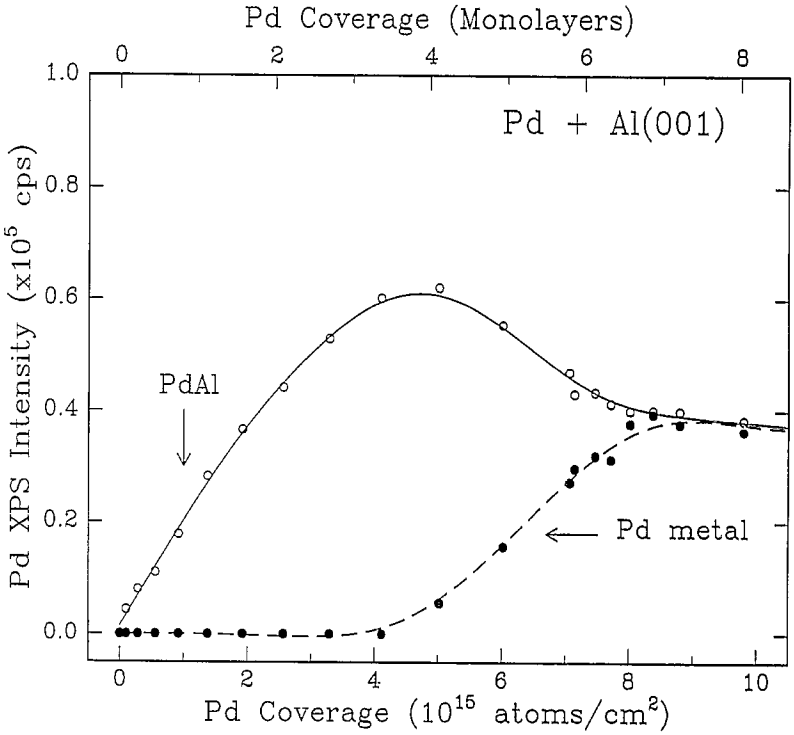

Fig. 6. Measured XPS intensity for the Pd $3d_{5/2}$ photopeak as a function of Pd coverage. The open circles (solid line) show the intensity for Pd photoelectrons coming from the AlPd alloy. The solid circles (dashed line) show the estimated emission intensity for Pd photoelectrons originating *only* from the metal film on the sample. The lines are provided to guide the eye.

cess has no effect on the Pd compound curve since this signal is coming only from the Al–Pd interface. A similar behavior in intensity is observed for the Pd $3d_{3/2}$ peak. Hence, the XPS peak shape analysis supports the model suggested by the ion scattering results.

Finally, we compare the above results for Pd films on Al(001) with those for Pd and Ni films on other Al surfaces. As mentioned earlier, we might expect the behavior of the Al–Pd and Al–Ni systems to be similar because of the similarities in their bulk phase diagrams. However, this is not the case. In our studies of ultrathin Ni films on the Al(001) surface, using HEIS, XPS and X-ray photoelectron diffraction (XPD), we observed that at low Ni coverages there is very little disruption of the Al surface and it appears that the Ni grows in small islands [4]. After 5 ML of Ni coverage the islands coalesce to cover the Al surface. For larger Ni coverages the Al SPA begins to increase, suggesting that a surface alloy may be forming. On the other hand, the growth of Ni films on Al(110) surfaces results in alloy formation at the surface for low Ni coverages as well, similar to the behavior of Pd on Al(100) [4]. Previous experiments for Pd on Al(111) using medium energy ion scattering, and our recent experiments for Pd on Al(110) using high energy ion scattering, show that there is considerable mixing at the Al–Pd interface [9,16]. We believe that a major factor in understanding the behavior for Ni and Pd films on Al surfaces is that the heat of formation for AlPd is relatively large, being -92 kJ/mole, whereas for AlNi it is only -59 kJ/mole [17]. A secondary factor may be that the Al(110) surface is relatively open and has the highest surface energy of the three low index faces. The surface energy of the Al(001) surface is about 10% less than that of the Al(110) surface, and that for the Al(111) surface is even lower [18]. This combination of chemical and structural parameters may be sufficient to explain the variety of growth modes for Ni and Pd on the various Al surfaces.

5. Conclusion

In summary, we have performed high energy ion scattering and X-ray photoelectron experiments for thin Pd films deposited on the Al(001) surface at room temperature. Initially, deposited Pd atoms displaced the Al atoms indicating a strong mixing between the Pd and Al atoms. For the first 5 ML of deposited Pd an AlPd-like alloy is formed. The mixing continues up to 5 ML of Pd coverage, at which point a Pd metal film begins to grow on the surface. The XPS measurements of the Pd 3d photopeaks show a chemical shift that is consistent with the formation of AlPd during the mixing stage, and Pd metal thereafter. The coverage dependence of the XPS intensities also supports this two-stage mixing model. From this work and related studies we further conclude that Pd deposition results in Al–Pd alloy formation on all low-index Al surfaces.

Acknowledgements

We are pleased to acknowledge the technical support of Erik Andersen and Norm Williams. This work was supported by the Montana Space Grant Consortium, NASA Grant No. GT40041, and by NSF Grant No. DMR-9409205.

References

[1] W.F. Smith, Structure and Properties of Engineering Alloys (McGraw-Hill, New York, 1981).
[2] T. Sands, Appl. Phys. Lett. 52 (1988) 197.
[3] Adli A. Saleh, V. Shutthanandan and R.J. Smith, Phys. Rev. B 49 (1994) 4908.
[4] V. Shutthanandan, Adli A. Saleh and R.J. Smith, J. Vac. Sci. Technol. A 1 (1993) 1780; V. Shutthanandan, PhD Thesis, Montana State University, 1994.
[5] N.R. Shivaparan, V. Shutthanandan, V. Krasemann and R.J. Smith, Bull. Amer. Phys. Soc. 40 (1995) 593.
[6] M. Hansen, Constitution of Binary Alloys, Ed. K. Anderko (McGraw-Hill, New York, 1958).
[7] B. Frick and K. Jacobi, Phys. Rev. B 37 (1988) 4408.
[8] Xu Mingde and R.J. Smith, J. Vac. Sci. Technol. A 6 (1988) 739.
[9] R.J. Smith, A.W. Denier van der Gon and J.F. van der Veen, Surf. Sci. 233 (1990) 103.
[10] U. Koster, P.S. Ho and M. Ron, Thin Solid Films 67 (1980) 35.
[11] E.G. Colgan, J. Appl. Phys. 62 (1987) 2269.
[12] R.J. Smith, C.N. Whang, Xu Mingde, M. Worthington,

C. Hennesy, M. Kim and N. Holland, Rev. Sci. Instrum., 58(12) (1987) 2284.
[13] E.J. van Loenen, M. Iwami, R.M. Tromp and J.F. van der Veen, Surf. Sci. 137 (1984) 1; E.J. van Loenen, J.F. van der Veen and F.K. LeGoues, Surf. Sci. 157 (1985) 1.
[14] V. Shutthanandan, Adli. A. Saleh, A.W. Denier van der Gon and R.J. Smith, Phys. Rev. B 48 (1993) 18292.
[15] F.U. Hillerbrecht, J.C. Fuggle, P.A. Bennett, Zygmunt Zolnirek and Ch. Freiburg, Phys. Rev. B 27 (1983) 2179.
[16] V. Shutthanandan, N.R. Shivaparan and R.J. Smith, unpublished.
[17] F.R. de Boer, R. Boon, W.C.M. Mattens, A.R. Miedema and A.K. Niessen, Cohesion in Metals: Transition Metal Alloys (North-Holland, Amsterdam, 1988).
[18] S.P. Chen, A.F. Voter, R.C. Albers, A.M. Boring and P.J. Hay, J. Mater. Res. 5 (1990) 955.